JOURNAL OF MATERIALS SCIENCE **34** (1999) 1557–1571

Densification of a rapidly solidified nickel aluminide powder

Part II *Characterization of microstructure and mechanical properties*

J. DUSZCZYK
Laboratory for Materials Science, Delft University of Technology, Rotterdamseweg 137, 2628 AL Delft, The Netherlands

L. Z. ZHUANG
Hoogovens Group, Research and Development, 1970 CA IJmuiden, The Netherlands

L. BUEKENHOUT
Bodycote Industrial Materials Technology, Industriepark-Noord 7, B-9100 Sint-Niklaas, Belgium

A Ni_3Al–X intermetallic compound prepared from a rapidly solidified powder was consolidated with hot isostatic pressing (HIP). Its microstructural development during the process has been examined. It involves a change from an inhomogeneous structure (a mixture of dendritic and equiaxed structures) to a uniformly distributed equiaxed structure and the formation of a disordered γ network phase from a metastably ordered matrix supersaturated with chromium, as a result of non-equilibrium solidification of the powder. The resulting microstructure of the consolidated material is mainly a function of HIP temperature. Mechanical properties of the HIP material at room and elevated temperatures have been determined. The results show that both the hardness and yield strength of the material decrease, while both the ultimate tensile strength and tensile elongation increase with rising HIP temperature up to 1250 °C. Scanning electron microscope examination of the fracture surfaces of tested samples reveals a transition from interparticle fracture to transparticle fracture with increasing HIP temperature.

1. Introduction

The intermetallic compound Ni_3Al has been considered a good candidate material for structural applications at elevated temperatures, due to its unusual characteristic mechanical property (i.e. the increase of flow stress with rising temperature up to about 700 °C) and good oxidation resistance [1, 2]. It becomes more attractive when the problem of its low-temperature brittleness can be solved through boron modification [3–6]. Significant improvements in ductility have been observed in the boron-modified materials prepared with both powder metallurgy (PM) and casting techniques [3, 4]. However, PM starting with powder production involving rapid solidification offers a number of unique advantages that are important to the ductility of the material. For example, segregation in the powdered material can be minimized (or no macrosegregation could occur in the compacted powder), very fine grains can be produced, and the solid solubility of alloying elements increased [7]. A possible disadvantage is, however, that surface contamination of the powder could lead to undesirable properties [8–10]. At present, a lot of effort is being made to improve the mechanical properties of the material and to scale-up a feasible method of fabricating PM components. A critical step in PM fabrication is the consolidation of a rapidly solidified powder.

Hot isostatic pressing (HIP), utilizing a combination of elevated temperature and isostatic gas pressure to consolidate powder [11, 12], plays an important role in PM fabrication. It is versatile and its commercial applications include the fabrication of high-quality metallic and ceramic components, which are otherwise difficult to make. Moreover, the process enables the powder to be consolidated into near-net-shape components, thereby maximizing material utilization. It is well known that Ni_3Al-based intermetallic compounds are generally brittle at low temperatures and difficult to hot work due to their unusual temperature–property response, although components with useful properties have successfully been produced. Therefore, the HIP process is specially useful in the fabrication of PM Ni_3Al-based intermetallic components [13–19].

In Part I of this communication [20], the densification behaviour of a Ni_3Al–X intermetallic powder during

HIP has been reported. It is shown that the constructed HIP maps generally agree with the experimental results. However, deviations have been observed in the low-temperature power-law creep region, and also in the high-temperature short-time HIP cycles. These have been attributed to the special property–temperature dependence exhibited by this intermetallic. In Part II, the results of microstructural examination of the HIP material as well as its mechanical properties at room and elevated temperatures will be presented. The influence of HIP variables on microstructural development and mechanical properties of the consolidated material will be discussed.

2. Experimental procedure

The material used in the present study was a modified Ni_3Al intermetallic compound containing boron, zirconium and chromium. Its chemical composition together with impurities is given in Table I. The powder (GAPDRY plant, Höganäs AB, Sweden) was prepared from a master alloy by using induction melting in an argon atmosphere and then argon atomization. Powder particles larger than 250 μm were discarded. The sieved powder had a volume mean diameter of 75.7 μm and a spherical shape. More detailed information about the powder can be found in [20].

Prior to consolidation, the powder was poured into stainless steel tubes with a diameter of 20 mm, a thickness of 2 mm and a length of 600 mm under argon protection and then sealed. The canned powder was consolidated with the HIP process under varying conditions at Bodycote Industrial Materials Technology, Belgium. Most of the experiments were performed using a laboratory-scale HIP unit having a cylindrical sample chamber with a diameter of 100 mm and a height of 200 mm. But in order to prepare samples for the evaluation of mechanical properties, a larger HIP unit with a diameter of 250 mm and a length of 750 mm was used. In the first set of HIP experiments, temperatures of 850, 950, 1050, 1150, 1250 and 1330 °C were used, while the applied pressure was kept constant at 100 MPa and the time at 30 or 120 min. In the second set of HIP experiments, the pressure varied from 5 to 150 MPa, while the temperature was fixed at 950 or 1150 °C and the time at 30 or 120 min.

TABLE I Analysed chemical composition and impurity levels in the atomized powder (wt %, but p.p.m. for N, H and O)

Al	Ni	Zr	Cr	B	Si	C	S	N	H	O
8.32	Balance	0.94	7.41	0.030	0.008	0.010	$\leq$0.005	75	41	148

The microstructure of the HIP intermetallic was studied by optical microscopy (OM) and transmission electron microscopy (TEM). OM specimens were etched with a solution consisting of 85% acetic acid, 8% HNO_3, 2% HF and 5% glycerol by volume. Disc-shaped TEM specimens were thinned with jet polishing in an electrolyte with 7.5% perchloric acid, 10% butyl cellosolve, 70% ethanol and 12.5% distilled water, by volume, at a temperature between −20 and −30 °C and a potential of 30 V. TEM specimens were examined in a Philips EM 400T or CM 30T microscope.

Vickers hardness was measured on polished surfaces of specimens cut from HIP bars. Tensile properties of the intermetallic HIP at 100 MPa and various temperatures (850, 950, 1050, 1150, 1250 and 1330 °C) were determined at room and elevated temperatures up to 950 °C. Tensile tests were performed at a constant cross-head speed of 1.494 mm min^{-1} (corresponding to an initial strain rate of 8.3×10^{-4} s^{-1}) using a screw-driven TTC-ML Instron machine equipped with a computer-assisted strain monitor. The samples were cylindrical with a gauge length of 30 mm and a diameter of 6 mm. Fracture surfaces of tested samples were examined by scanning electron microscopy (SEM).

3. Results and discussion

3.1. Microstructure of the atomized powder

Optical microstructure of sectioned powder particles is shown in Fig. 1. Fig. 1a is a low-magnification micrograph, which gives a general view of the microstructure of this atomized powder. Details of the microstructural characteristics of the powder, i.e. having both dendritic and equiaxed structures, can be seen in Fig. 1b at higher magnification. Although the metallographic sections may not reveal the real particle diameters, an approximate representation of the size distribution of powder particles can be obtained when a relatively large number

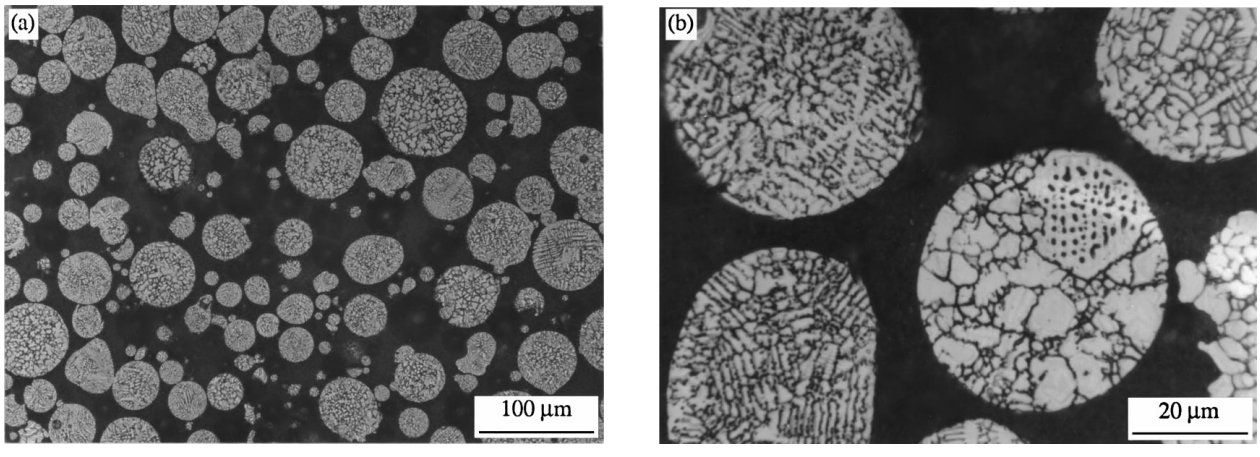

Figure 1 Optical micrographs showing both dendritic and equiaxed structures in the powder.

of powder particles are taken into account. It has been observed that there is no dependency of structure (dendritic or equiaxed) or dendrite spacing on particle size and thus on the atomization cooling rate; different microstructures and different dendritic spacings can be found in both large and small particles and even within the same particle. Moreover, the relative amounts of dendritic and equiaxed structures are also independent of particle size. This result is not in agreement with the general observation of the relationship between microstructure and particle size reported in other materials [6, 7, 9, 10].

TEM reveals that the as-atomized material has essentially a single-phase structure. Unlike the microstructures observed in the same material prepared with the Osprey spray-deposition and casting processes [21–24], no disordered γ network structure can be found in the atomized powder, except certain disordering at grain boundaries. The volume fraction of the disordered γ phase in the powdered material is very low, probably less than 1–2%, as contrasted to that in the Osprey-spray-deposited or ingot-cast materials (up to approximately 10–15%). Therefore, the as-atomized powder is characterized by a microstructure consisting mainly of a metastably ordered phase with a supersaturated concentration of the A type constituent (in A_3B structure) resulting from non-equilibrium solidification. The antiphase domain (APD) structure in the grain interior has been observed in the atomized powder, as shown in Fig. 2. In this figure, discrete γ' domains of 80–100 nm in size are separated by antiphase boundaries.

3.2. Microstructural characterization of the HIP material

Microstructural evolution in the present intermetallic during HIP is complicated because the atomized powder particles have a metastably ordered structure supersaturated with chromium as a result of non-equilibrium solidification. It involves a change in characteristic microstructure from a rapidly solidified, inhomogeneous structure (a mixture of dendritic and equiaxed structures) to a uniformly distributed equiaxed structure and the formation of the disordered γ network phase from the metastably ordered matrix.

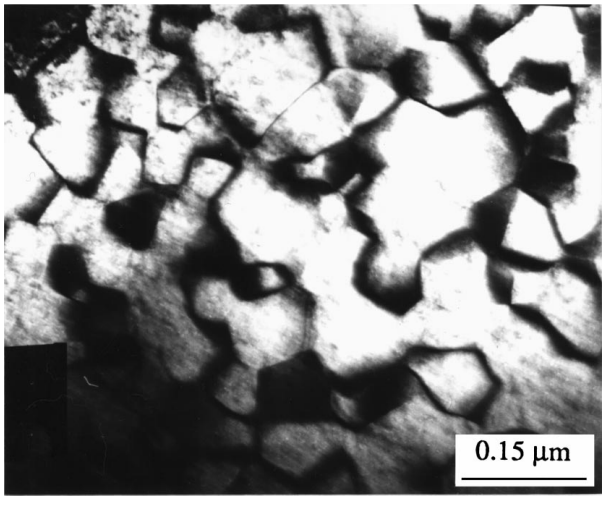

Figure 2 TEM dark field micrograph showing the APD structure in the atomized powder.

The dependence of the microstructure of the intermetallic on the HIP temperature between 850 and 1330 °C has been shown in [20] (see Fig. 8 therein). The microstructure of the HIP material can be divided into three categories:

1. When the material is subjected to HIP at temperatures below 950 °C, its microstructure is about the same as that observed in the as-atomized powder. After HIP, each powder particle retains its own identity and characteristic microstructure, as shown in Fig. 8a and b for the material subjected to HIP at 850 and 900 °C, respectively.
2. With increasing HIP temperature, homogenization and recrystallization of the matrix and formation of the disordered γ phase in the metastably ordered γ' phase are in progress. Even when a HIP temperature of 1150 °C is reached, the above-mentioned microstructural development is not completed yet. The heterogeneous nature of the powder, i.e. different types of structure (dendritic and equiaxed) within individual particles, partially remains, as shown in Fig. 8c and d for the material subjected to HIP at 1050 and 1150 °C, respectively.
3. When the material is subjected to HIP at temperatures above 1250 °C, a uniformly distributed equiaxed structure with a coarser grain size is formed. A well developed γ/γ' network structure can be observed within individual particles, as shown in Fig. 8e and f. It is interesting to note that the average size of the γ/γ' network structure in the HIP material at 1250 and 1330 °C is about the same. This implies that the network size of the γ/γ' structure under an equilibrium condition is presumably only composition sensitive but not temperature sensitive. Original particle boundaries can still be discerned in the material because of the bimodal distribution of the disordered γ phase resulting from segregation, similar to that observed in the Osprey-spray-deposited material [21, 22]. Usually, a fine equiaxed γ/γ' network structure is observed in the particle interior and a coarser equiaxed γ/γ' network structure or a radial structure at the particle boundaries. In addition, the powder particles in the material subjected to HIP at 1330 °C are no longer spherical because the intermetallic becomes very soft at this temperature and undergoes heavy deformation during HIP. However, the powder particles in the material subjected to HIP at lower temperatures remain spherical.

The newly, incompletely developed microstructure of the material subjected to HIP at low temperatures is very fine; that subjected to HIP at 1050 and 1150 °C even shows a featureless structure in OM at high magnifications. Fig. 3 shows the microstructures of the HIP material with differential interference contrast (DIC) in order to improve the contrast of the micrographs and thus to reveal all the characteristic microstructures, such as dendrites, grain boundaries and γ/γ' network

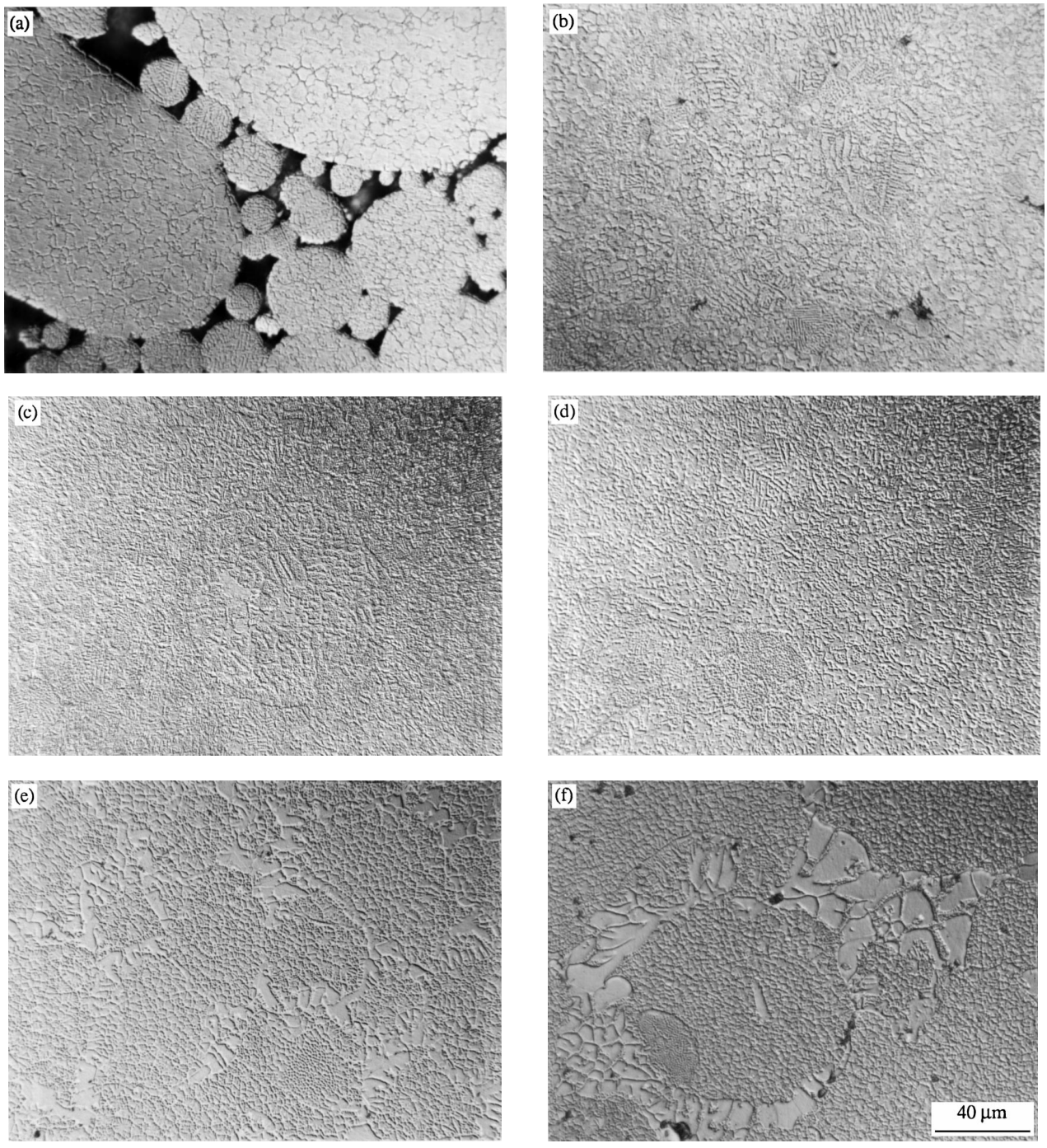

Figure 3 Optical (DIC) micrographs showing the microstructures developed in the material subjected to HIP at 100 MPa and at temperatures of (a) 850, (b) 950, (c) 1050, (d) 1150, (e) 1250, and (f) 1330 °C.

structure. However, due to the fineness of the microstructure of the material subjected to HIP at 1050 and 1150 °C, the DIC micrographs with a magnification of ×500 are still not clear enough to show the details of microstructural features. Fig. 4 gives a set of DIC micrographs taken from the HIP material with a magnification of ×2000, which show more details of its microstructure. In the material subjected to HIP at 850 and 950 °C, no disordered γ phase can be observed in the grain interior, see Fig. 4a and b. In the material subjected to HIP at 1050 and 1150 °C, a certain amount of the disordered γ phase is present in the grain interior but it is not connected to form a γ/γ' network structure, as shown in Fig. 4c and d. In the material subjected to HIP at 1250 and 1330 °C, as discussed earlier, a well developed γ/γ' network (or radial) structure is observed, see in Fig. 4e and f, showing the microstructure in the areas containing the original particle boundaries.

From OM examination of the HIP material, it is also noted that large powder particles usually retain a high degree of residual sphericity, as can be seen in Fig. 8d in [20]. This implies that the large particles have experienced less deformation than small ones during HIP. Such particles exhibit a much coarser microstructure, as shown in Fig. 8d [20] and Fig. 5, which suggests that less microstructural change has taken place. This observation is similar to that reported by Kaysser *et al*. [25] with regard to the effect of particle size and deformation on the microstructural development within individual particles during HIP.

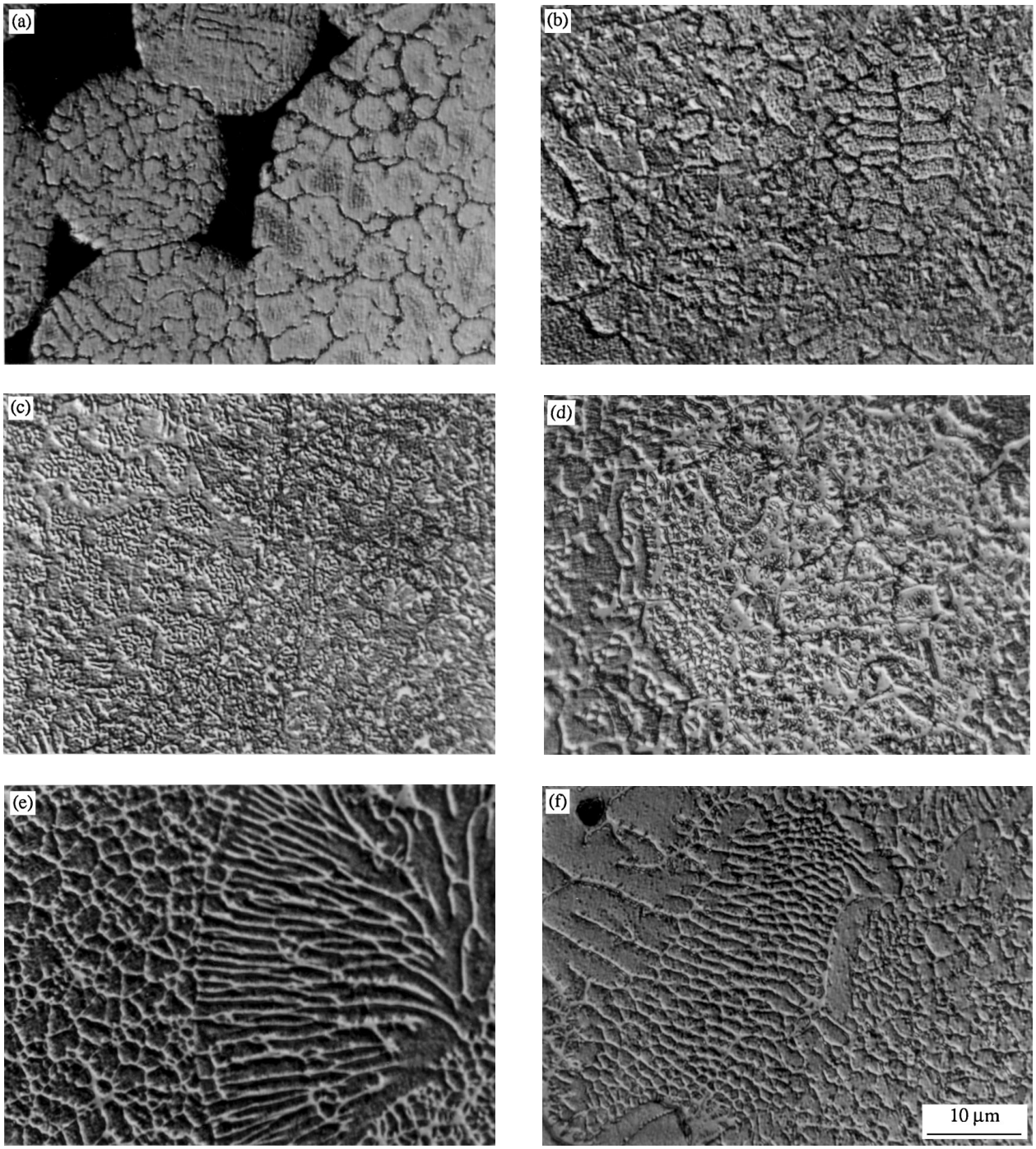

Figure 4 High-magnification optical (DIC) micrographs showing details of the microstructures in the material subjected to HIP at 100 MPa and at temperatures of (a) 850, (b) 950, (c) 1050, (d) 1150, (e) 1250, and (f) 1330 °C.

In addition, several defect structures have been observed in the HIP material. Fig. 6 is a micrograph taken from the material subjected to HIP at 1150 °C, showing internal cracks within an original powder particle. In the material subjected to HIP at low temperatures, similar defect structures have also been observed. However, in the material subjected to HIP at 1250 and 1330 °C, such internal cracks have not been found. These internal cracks presumably result from enclosed gas bubbles or pores in some of the atomized powder particles. These pores may break down to form the internal cracks when the powder is subjected to HIP at a certain temperature and pressure. When hot isostatically pressed at a higher temperature or pressure, the powder particles would undergo higher deformation so that the enclosed gas bubbles or pores would be broken down and then closed completely. In the material subjected to HIP at 1330 °C, incipient interparticle melting is observed, as shown in Fig. 7. The melted material usually forms much thicker γ/γ' boundaries. During cooling from the HIP temperature, a mixed microstructure of the disordered γ phase and secondary precipitated γ' particles is formed at these boundaries. In addition, a considerable amount of oxide particles mostly located at the original powder particle boundaries is observed in the material subjected to HIP at 1330 °C, as shown in Fig. 8. These oxide particles are formed during hot isostatic

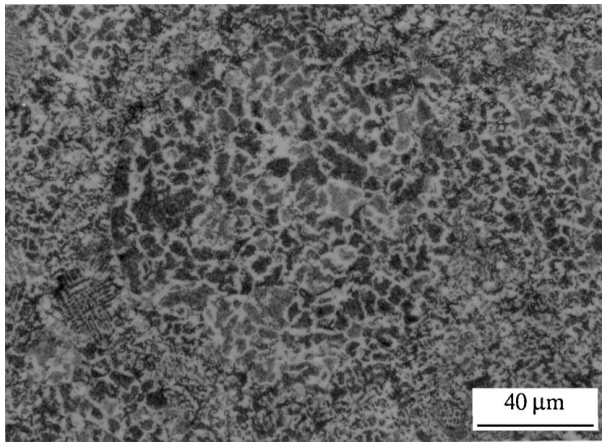

Figure 5 Optical micrograph showing a large, less deformed particle in the 1050 ° HIP material.

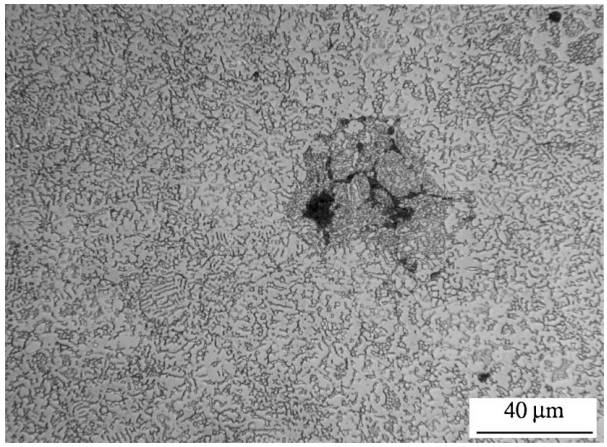

Figure 6 Optical micrograph showing internal cracks within a powder particle in the HIP material.

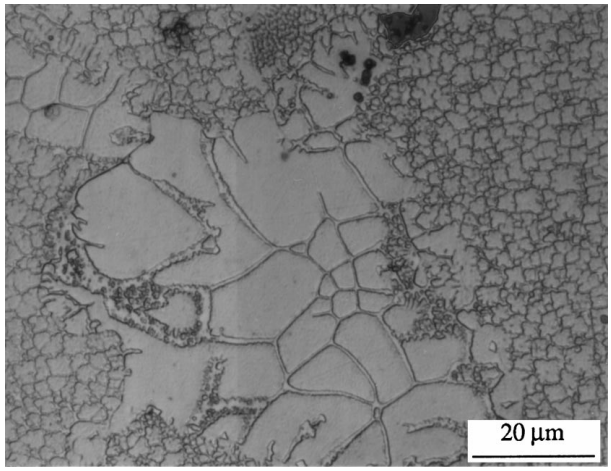

Figure 7 Optical micrograph showing incipient interparticle melting in the 1330 °C HIP material.

pressing at this high temperature, as they have not been found in the material subjected to HIP at lower temperatures.

As discussed above, HIP temperature is a major factor influencing the microstructure of the HIP material, while HIP pressure exerts far less influence. For instance, no evident differences in microstructure can be found in the material consolidated with various pressures at 1150 °C, as shown in Fig. 9.

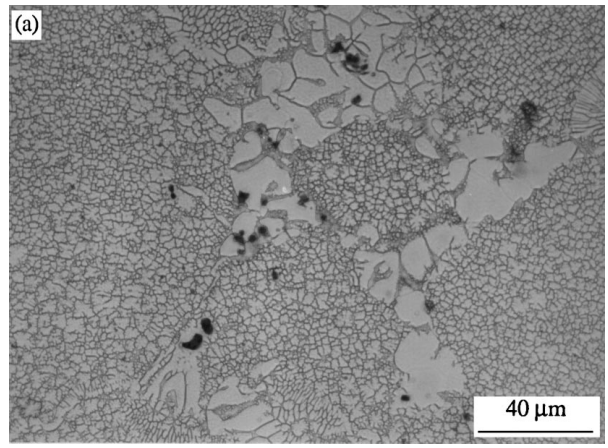

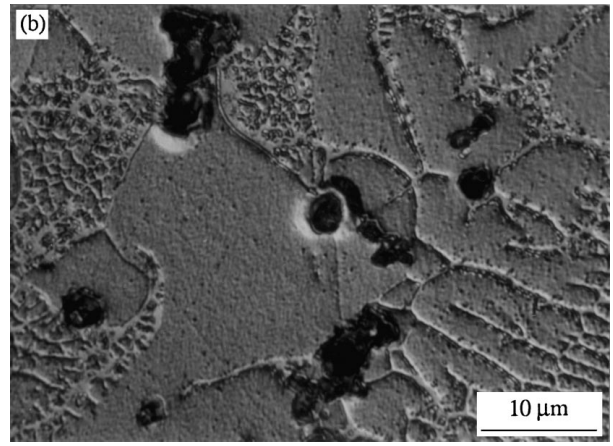

Figure 8 Optical micrographs showing process-introduced oxide particles in the material formed during HIP at 1330 °C. The oxide particles are mostly located at the original powder particle boundaries: (a) BF image, and (b) DIC image.

In addition to the OM-observed characteristic microstructure, TEM further reveals a fine grain structure in the material hot isostatic pressed at temperatures $\leq$1150 °C. Fig. 10 presents TEM bright field (BF) micrographs taken from the material subjected to HIP at 850 and 950 °C, showing a very fine structure with a grain size of approximately 3–5 μm. Also seen are deformation-introduced dense dislocations at grain boundaries and in the grain interior. Other structures associated with a thermomechanical process have also been found. Fig. 11 shows a deformation-induced twin boundary structure located at a grain junction, as observed in the material subjected to HIP at 950 °C.

A mixture of fine antiphase domains (APDs) in the central regions of grains and coarse APDs in the regions adjacent to grain boundaries within individual grains is observed in the material subjected to HIP at 850 and 950 °C (Fig. 12). This microstructural feature, i.e. APDs with a bimodal size distribution, is the same as that observed in the atomized powder [21]. Combined with the results obtained from OM examination, it is concluded that the characteristic microstructure of the atomized powder, both on a large scale (dendritic and equiaxed structures) and on a fine scale (APD structure), is mostly retained in the material subjected to HIP at 850 and 950 °C.

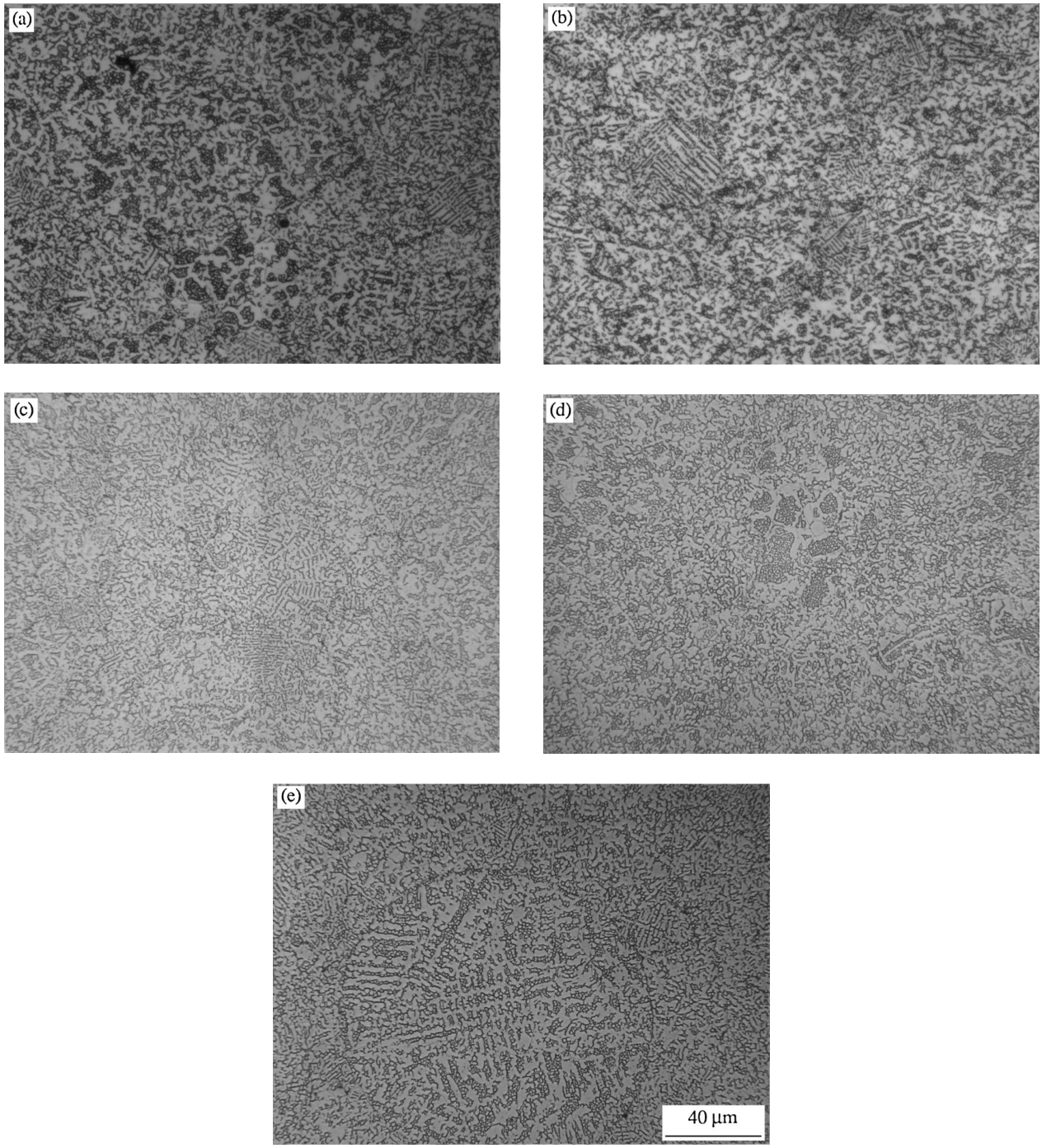

Figure 9 Optical micrographs showing microstructures developed in the material subjected to HIP at 1150 °C and at pressures of (a) 10, (b) 50, (c) 75, (d) 100, and (e) 150 MPa.

Fig. 13 presents a set of TEM dark field (DF) micrographs showing the microstructural evolution on a fine scale for the material subjected to HIP at different temperatures. Here, the changes in the APD structure and the formation of the disordered γ phase with increasing HIP temperature are demonstrated. It is clear that with increasing HIP temperature from 850 up to 1050 °C, Fig. 13a–c, the APD size increases, the morphology of the APD boundaries changes from a well defined crystallographic feature (Fig. 2) to a less crystallographic irregular one, and disordering at the APD boundaries increases. In the material subjected to HIP at 1050 °C a marked thickness of the disordered film at most of the APD boundaries can be detected and at some places a well developed disordered γ structure can be observed.

In the material subjected to HIP at higher temperatures (1150, 1250 and 1330 °C), no APD structure is observed. This indicates that the order–disorder transition temperature of the Cr-containing Ni_3Al intermetallic is much lower than its melting temperature, in contradiction to the results often reported for the Ni_3Al compound. The APD structure is also not observed in the HIP material because it has been cooled down very slowly after consolidation. Both of these speculations have been verified through quenching experiments on this alloy [26]. In these experiments, bulk samples were heated up to 1200, 1250, 1300 and 1330 °C, kept

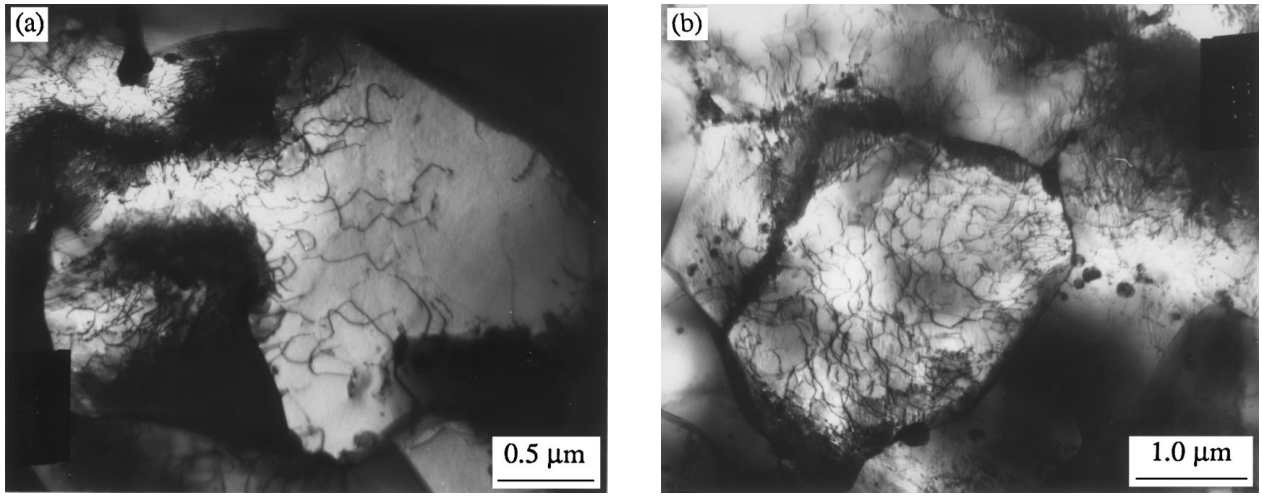

Figure 10 TEM bright field micrographs showing a fine grain structure with dense dislocations in the material subjected to HTP at (a) 850 and (b) 950 °C.

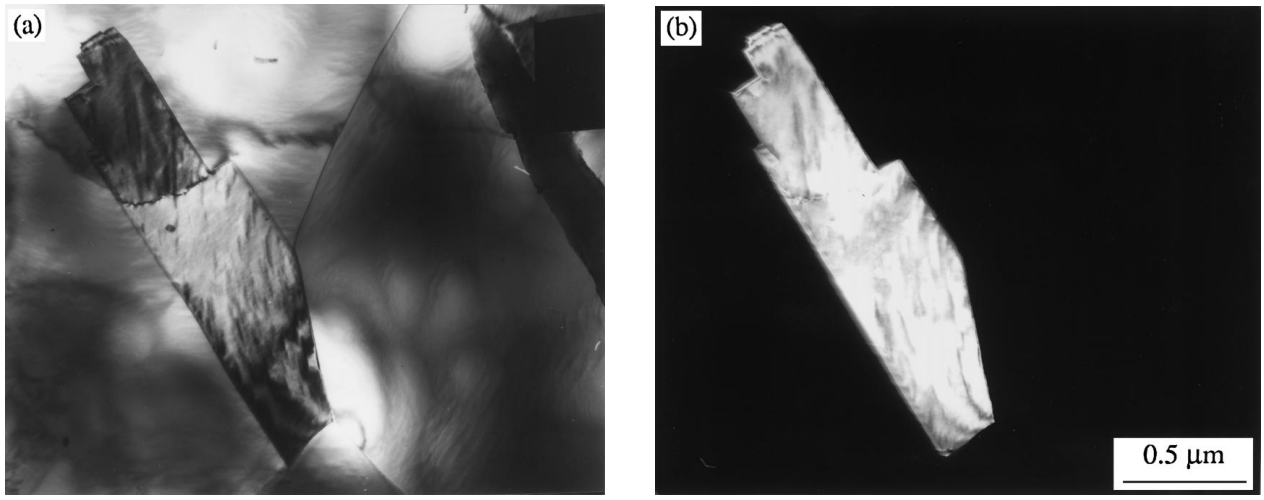

Figure 11 TEM micrographs showing a deformation-introduced twin boundary structure in the 950 ° HIP material: (a) BF image and (b) DF image formed using a twin reflection.

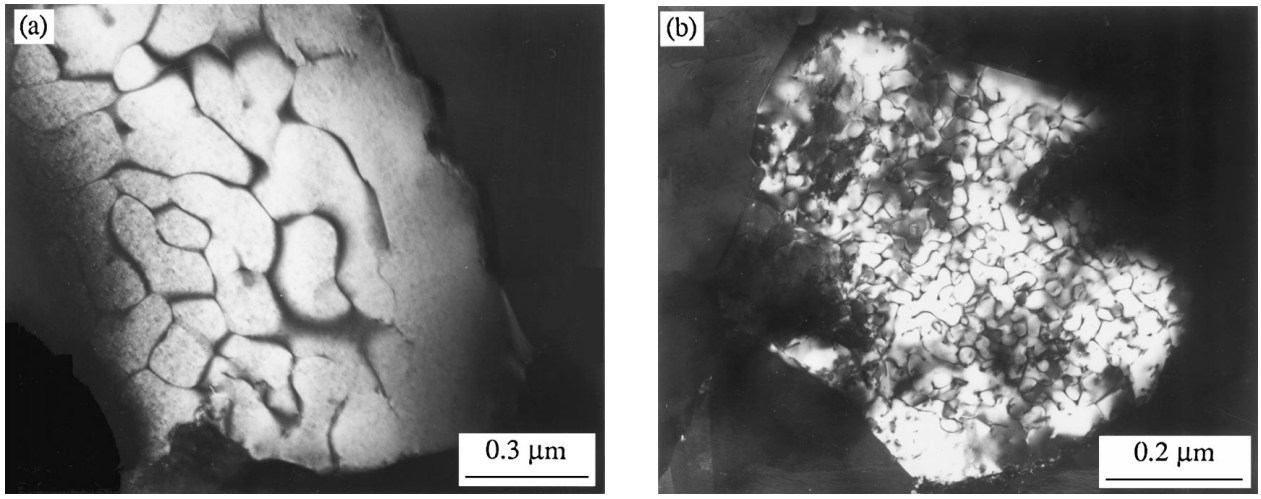

Figure 12 TEM dark field micrographs showing the APD structure and domain size distribution within individual grains in the material subjected to HIP at (a) 850 and (b) 950 °C.

for 2 h and then water quenched or furnace cooled. A newly formed fine network of APDs, resulting from a sequential ordering process [27], was observed in the quenched samples. When the sample was slowly cooled in a furnace from 1330 °C, although a sequential ordering process during cooling could be expected, no APD structure could be found. This result indicates that a low cooling rate will allow individual APD nuclei formed

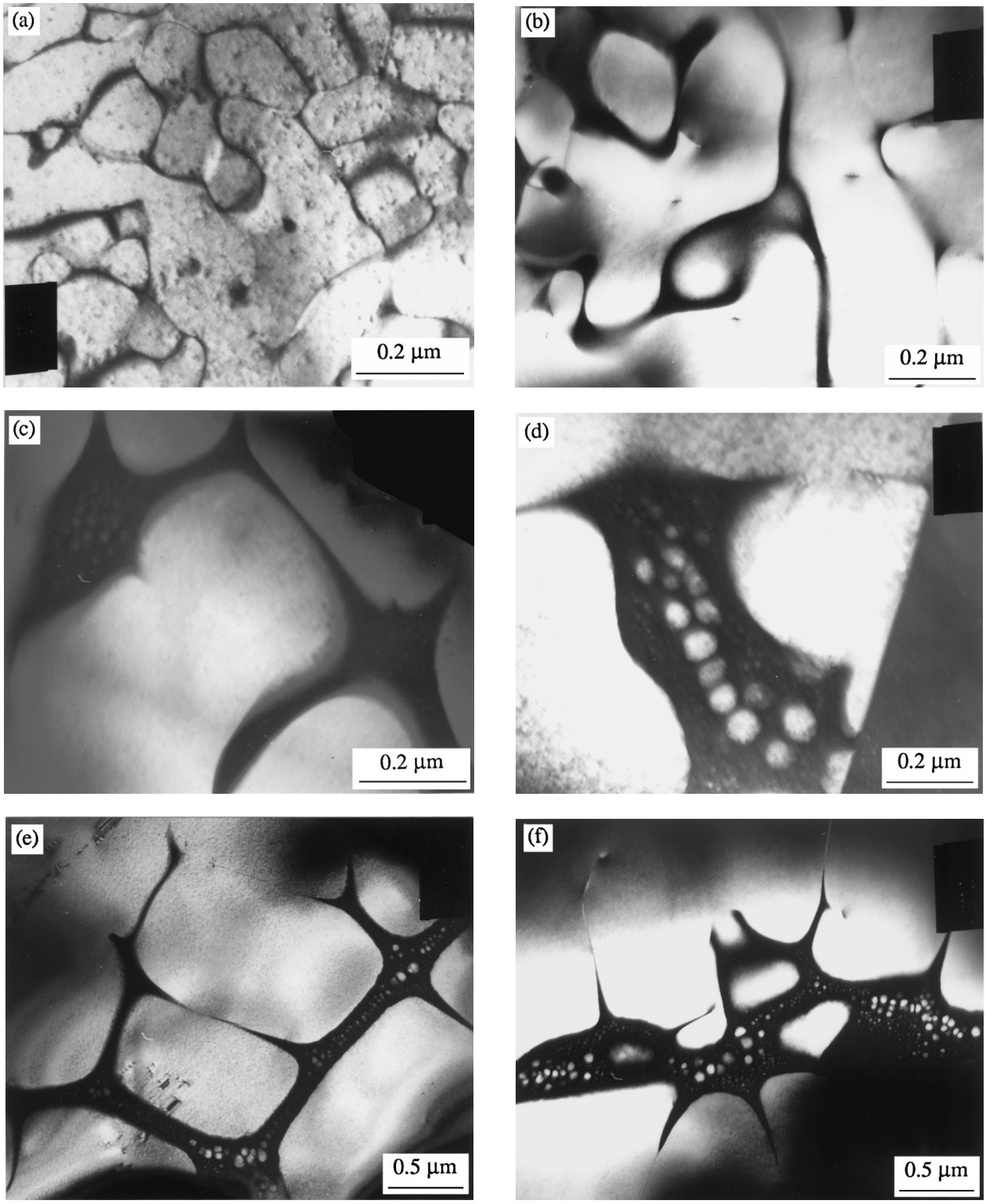

Figure 13 TEM dark field micrographs showing microstructure evolution in the material during HIP at 100 MPa and at temperatures of (a) 850, (b) 950, (c) 1050, (d) 115, (e) 1250, and (f) 1330 °C.

during cooling to grow up to a size of an entire grain or any other substructures. This could also be the case for the microstructural development in the material subjected to HIP at high temperatures.

As shown in Fig. 13d–f, extensive formation of the disordered γ phase has occurred in the material subjected to HIP at the temperatures between 1150 and 1330 °C. The disordered γ phase formed in the material subjected to HIP at 1150 °C usually has a discrete distribution and, therefore, no γ/γ' network structure can be observed. However, in the material subjected to HIP at 1250 and 1330 °C, a well established γ/γ' network structure can be seen. The thick parts of the disordered γ phase boundaries are usually filled with fine particles of the ordered γ' phase precipitated during cooling. This can be observed even in the material subjected to HIP at 1050 °C, as shown in Fig. 13c.

The formation of the disordered γ phase in the HIP material can be affected by microsegregation of alloying elements. This is demonstrated in Fig. 14a, in which

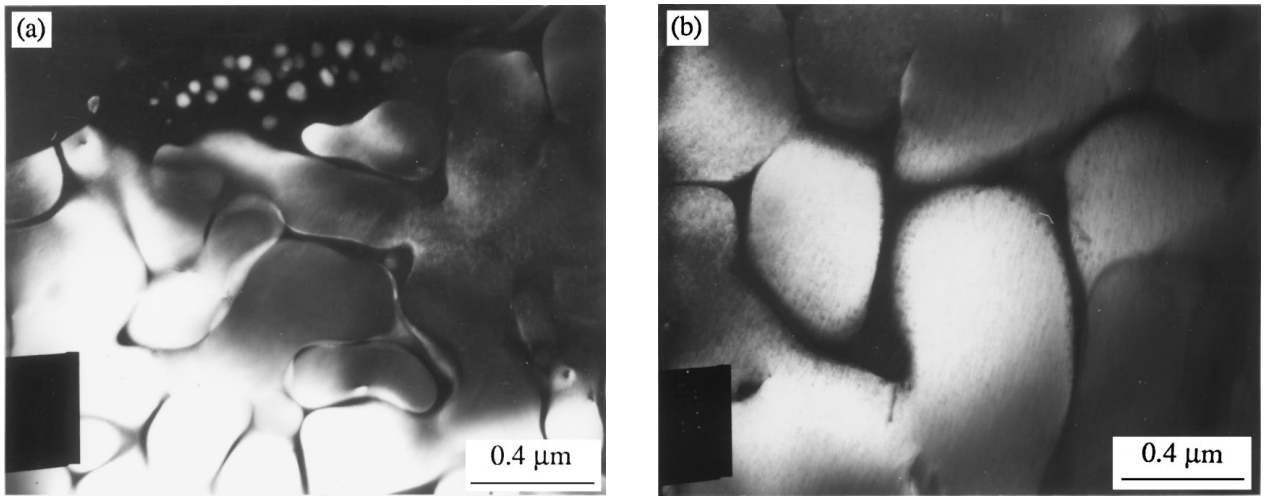

Figure 14 TEM dark field micrographs showing the effect of microsegregation on the formation of a disordered γ phase in the material subjected to HIP at (a) 950 and (b) 1050 °C.

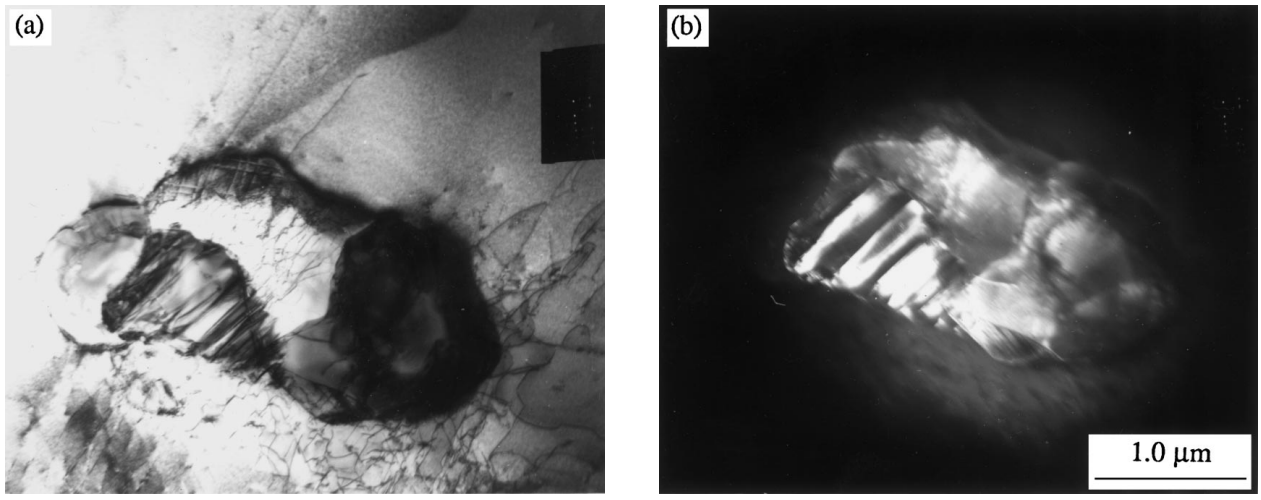

Figure 15 TEM micrographs showing an oxide particle observed in the 1330 °C HIP material: (a) BF image, and (b) DF image formed using a reflection from the oxide particle.

a well developed γ/γ' web (disordered γ phase filled with secondary precipitated γ' particles) in the material subjected to HIP at 950 °C can been seen. On the other hand, Fig. 14b shows a micrograph taken from a region that is essentially free of the disordered γ boundary in the material subjected to HIPed at 1050 °C.

Fig. 15 presents a set of micrographs with both the BF and DF images of an oxide particle observed in the material subjected to HIP at 1330 °C. The oxide particle surrounded by densely packed dislocations is formed at a grain boundary. The DF image is obtained by using a reflection from the oxide particle. A very fine powder particle with a diameter of less than 1 μm, observed in the material subjected to HIP at 1330 °C, is shown in Fig. 16 with both the BF and DF images. The crystal structure of the particle has not been identified, but it is not the regular $L1_2$ structure.

3.3. Mechanical properties of the HIP consolidated materials

Room-temperature hardness and tensile properties at room and elevated temperatures up 950 °C, of the material subjected to HIP at 100 MPa and different temperatures have been determined. The effect of HIP temperature on the mechanical properties of the material is shown in Figs 17 and 18. Fig. 17 shows the hardness values measured in the as-hot-isostatic-pressed material, which are the averages of at least six measurements. Fig. 18 presents its tensile property values, each of which is the average of three tests. The HIP material shows a good reproducibility in its mechanical properties; no evident differences in mechanical properties have been found between different samples (which were cut from different places of a HIP bar or from different HIP bars). Therefore, it can be concluded that HIP can indeed be used to prepare the Ni_3Al–X intermetallic material from its powder with a homogeneous microstructure or a homogeneous distribution of porosity if a low temperature is used.

The results show that a HIP temperature of 850 °C is obviously not adequate for proper processing of the material, as indicated by its low hardness value, tensile strength and ductility, because it has a very low relative density. In fact, microhardness measurement shows a very high hardness value of 345 VPN (Vickers

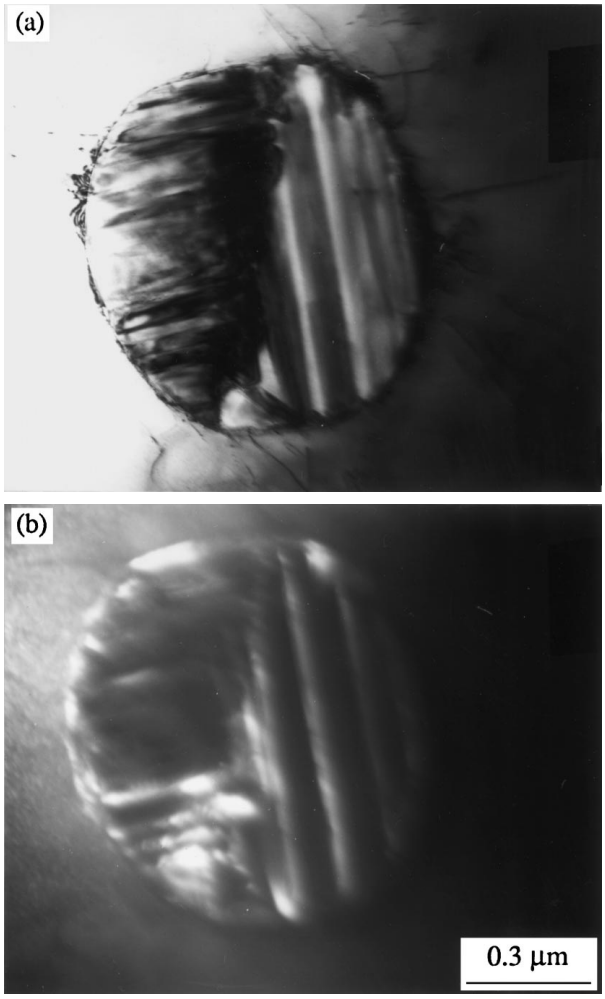

Figure 16 TEM micrographs showing the microstructure of a fine particle in the 1330 °C HIP material: (a) BF image, and (b) DF image formed using a reflection from the particle.

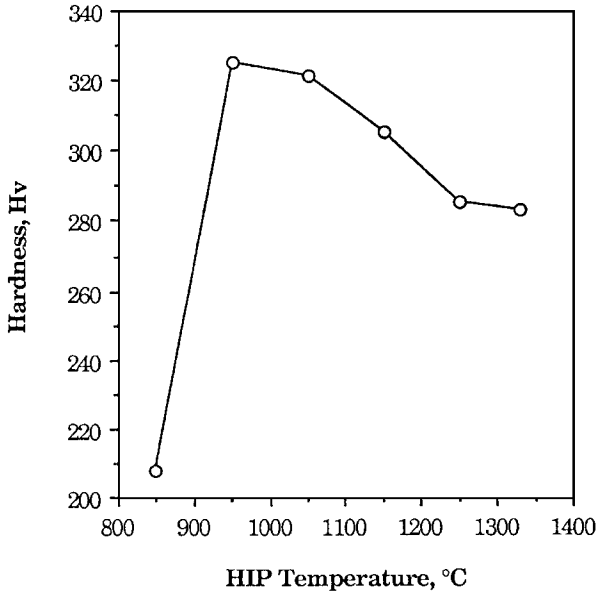

Figure 17 Relationship between the hardness, H_V, of the material and HIP temperature.

Pyramid Number) of the material after HIP. This value is lower than that measured from the as-atomized powder particles (369 VPN) but higher than those in the bulk material subjected to HIP at higher temperatures, as shown in Fig. 17.

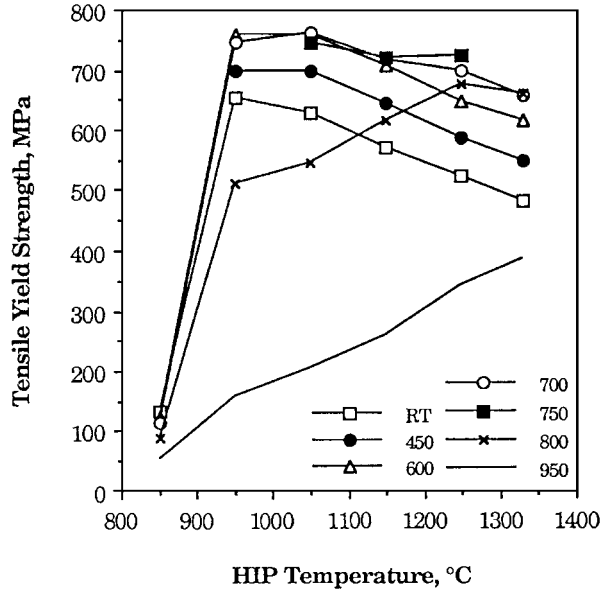

(a)

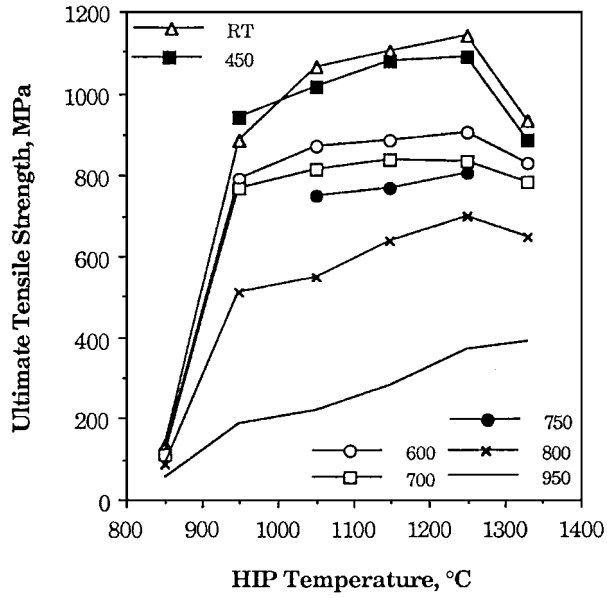

(b)

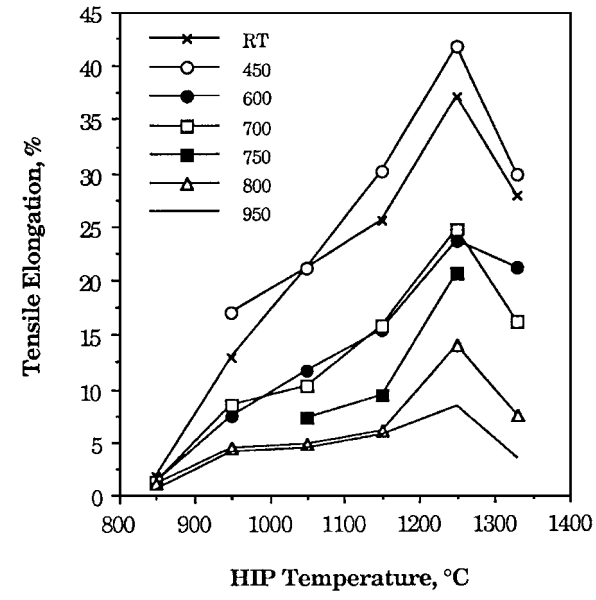

(c)

Figure 18 Relationship between the tensile mechanical properties of the material and HIP temperature: (a) tensile yield strength, (b) ultimate tensile strength, and (c) tensile elongation.

For the material subjected to HIP at temperatures $\geq$950 °C, the results indicate that the room-temperature hardness and the yield strength at temperatures below 750 °C decrease, while the ultimate tensile strength and tensile elongation as well as the yield strength at temperatures higher than 750 °C increase with increasing HIP temperature up to 1250 °C. These results are associated with the characteristic microstructure developed during HIP. The fineness of the microstructure is responsible for higher room-temperature hardness and yield strength (at temperatures <750 °C) of the material subjected to HIP at lower temperatures. Higher ultimate tensile strength and tensile elongation of the material subjected to HIP at higher temperatures are caused by the presence of a large amount of the disordered γ phase and also a homogeneous matrix microstructure. The material subjected to HIP at 1330 °C shows lower mechanical properties than that subjected to HIP at 1250 °C, especially its ultimate tensile strength and tensile ductility, due to the presence of some defect structures, such as incipient interparticle melting and oxide particles around the original powder particles, formed during HIP at this high temperature, as well as grain coarsening. However, the results obtained at testing temperatures >750 °C indicate that a higher HIP temperature, corresponding to a coarser structure, may be favourable for a higher yield strength of the intermetallic at high temperatures.

The relation between tensile properties and testing temperature is given in Fig. 19. The unusual yielding behaviour of the Cr-containing Ni_3Al-based powder consolidated by HIP, i.e. rising of the yield stress from room temperature to a temperature, T_p, and then falling at higher temperatures, is demonstrated in Fig. 19a. The peak temperature, T_p, at which the material reaches its highest yield stress, varies with HIP temperature. With increasing HIP temperature, it shifts to a higher temperature. In the present study, we find that T_p of the 950 °C HIP material is about 600 °C, while T_p of the 1330 °C HIP material is about 800 °C. The dependence of the tensile ductility of the HIP-consolidated intermetallic on temperature shows dynamic embrittlement at moderate temperatures (around 600 °C). Thus the ultimate tensile strength of the samples tested within this temperature region is also lower, although the yield strength of the intermetallic is in most cases the highest.

From the data shown in Fig. 18, it can be seen that the ultimate strength and tensile ductility of the alloy at testing temperatures up to 750 °C are consistent with each other; the ultimate strength increases with increasing elongation and vice versa. In fact, from the tensile load–extension (stress–strain) curves of the material, it has been found that the applied load after the yield point always shows a positive response to an increase in extension. Therefore, any factor that influences homogeneous plastic deformation between yielding and fracture will influence the ultimate tensile strength of the alloy. A homogeneous matrix microstructure with a fine grain or substructure size is important to the ultimate strength and ductility of the alloy. From the results of hardness and yield strength, one can see that the HIP material softens with increasing HIP temperature. The fact that the material subjected to HIP at 1250 °C has

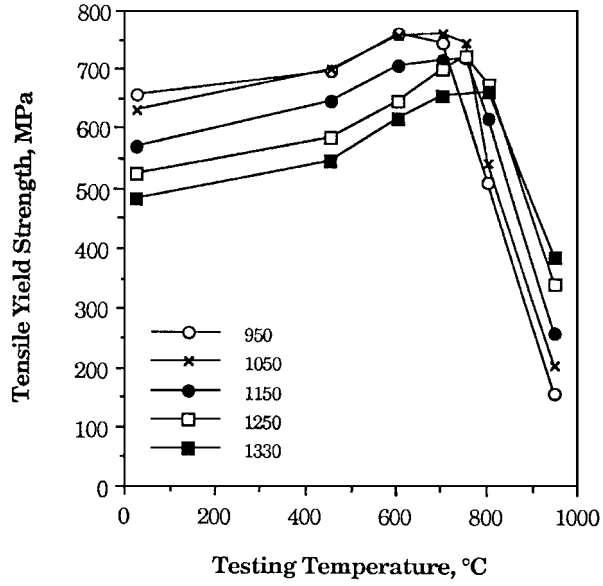

(a)

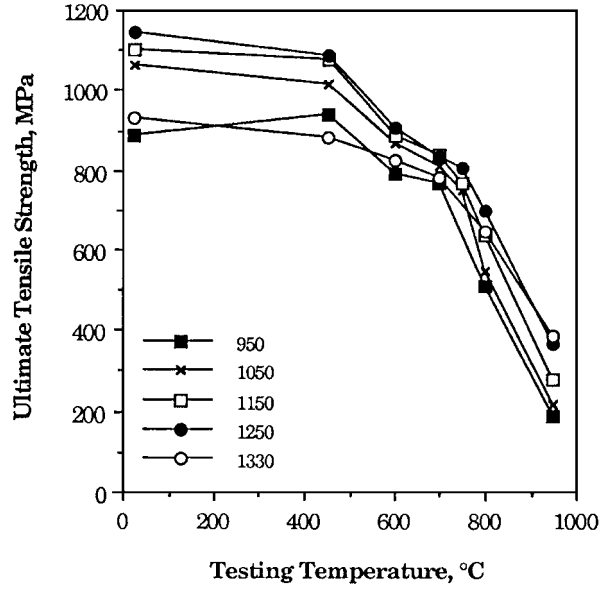

(b)

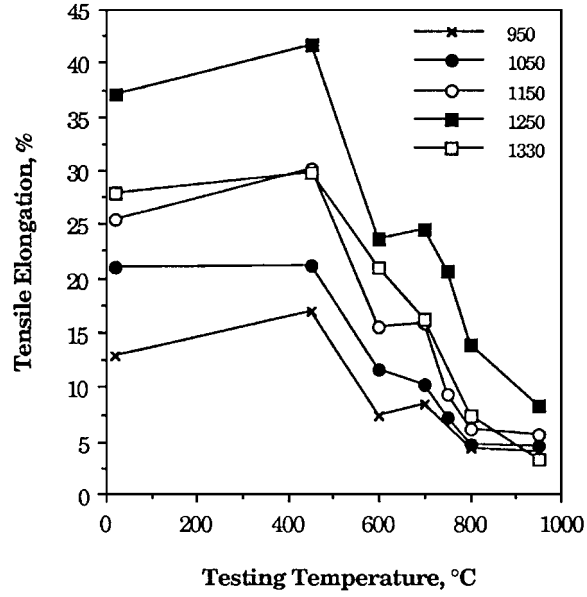

(c)

Figure 19 Relationship between the tensile mechanical properties of the HIP material and tensile-testing temperature: (a) tensile yield strength, (b) ultimate tensile strength, and (c) tensile elongation.

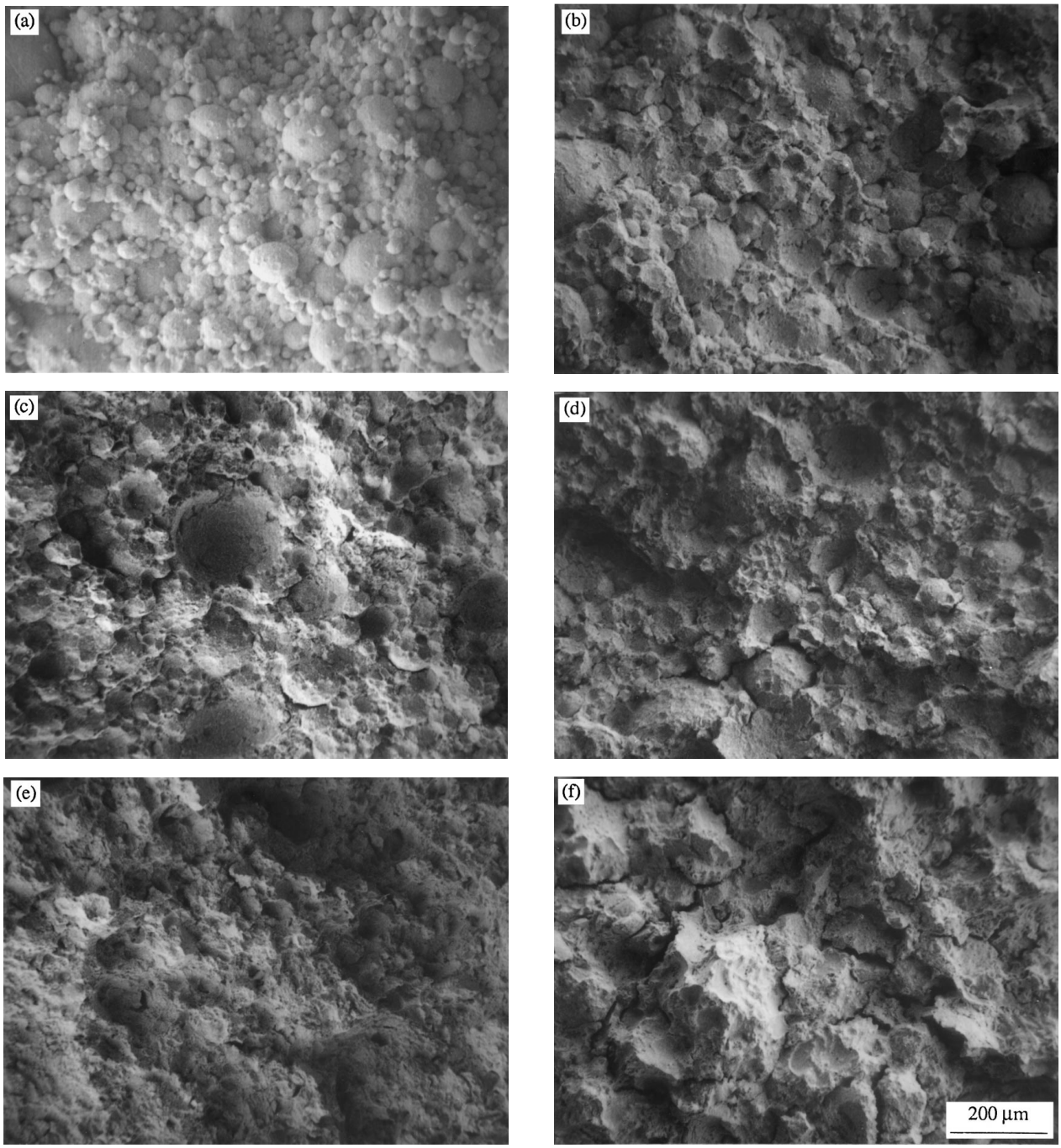

Figure 20 SEM micrographs showing a general view of the fracture morphology observed in the room-temperature tested material subjected to HIP at 100 MPa and at temperatures of (a) 850, (b) 950, (c) 1050, (d) 1150, (e) 1250, and (f) 1330 °C.

the highest ultimate strength and ductility is mainly due to its well homogenized matrix microstructure and a well developed γ/γ' network structure, which provides a very fine substructure size. This microstructure allows the material to undergo more homogeneous plastic deformation before fracture and thus to reach a higher tensile strength. The microstructure of the material subjected to HIP at lower temperatures is also fine, but metastable and inhomogeneous. In discussing the tensile properties of the present material, another important factor, interparticle bonding, must be considered. The interparticle bonding is probably a more important factor in determining the mechanical properties of the material consolidated at low temperatures. This can be seen from SEM fractographs of the tested samples.

Fig. 20 presents a set of SEM fractographs taken from the material subjected to HIP at 100 MPa and various temperatures, and tested at room temperature. They show a transition from interparticle fracture to transparticle fracture with increasing HIP temperature. A completely interparticle fracture morphology is observed in the material subjected to HIP at 850 °C and tested at various temperatures. For the material subjected to HIP at temperatures between 950 and 1150 °C, final rupture is predominantly in the interparticle fracture mode with mixed interparticle and transparticle fractures, indicating that interparticle bonding in the material is still not strong enough. The area fraction of transparticle fracture in the material increases with increasing HIP temperature. In the material subjected to HIP at 1250 and 1330 °C, no interparticle fracture

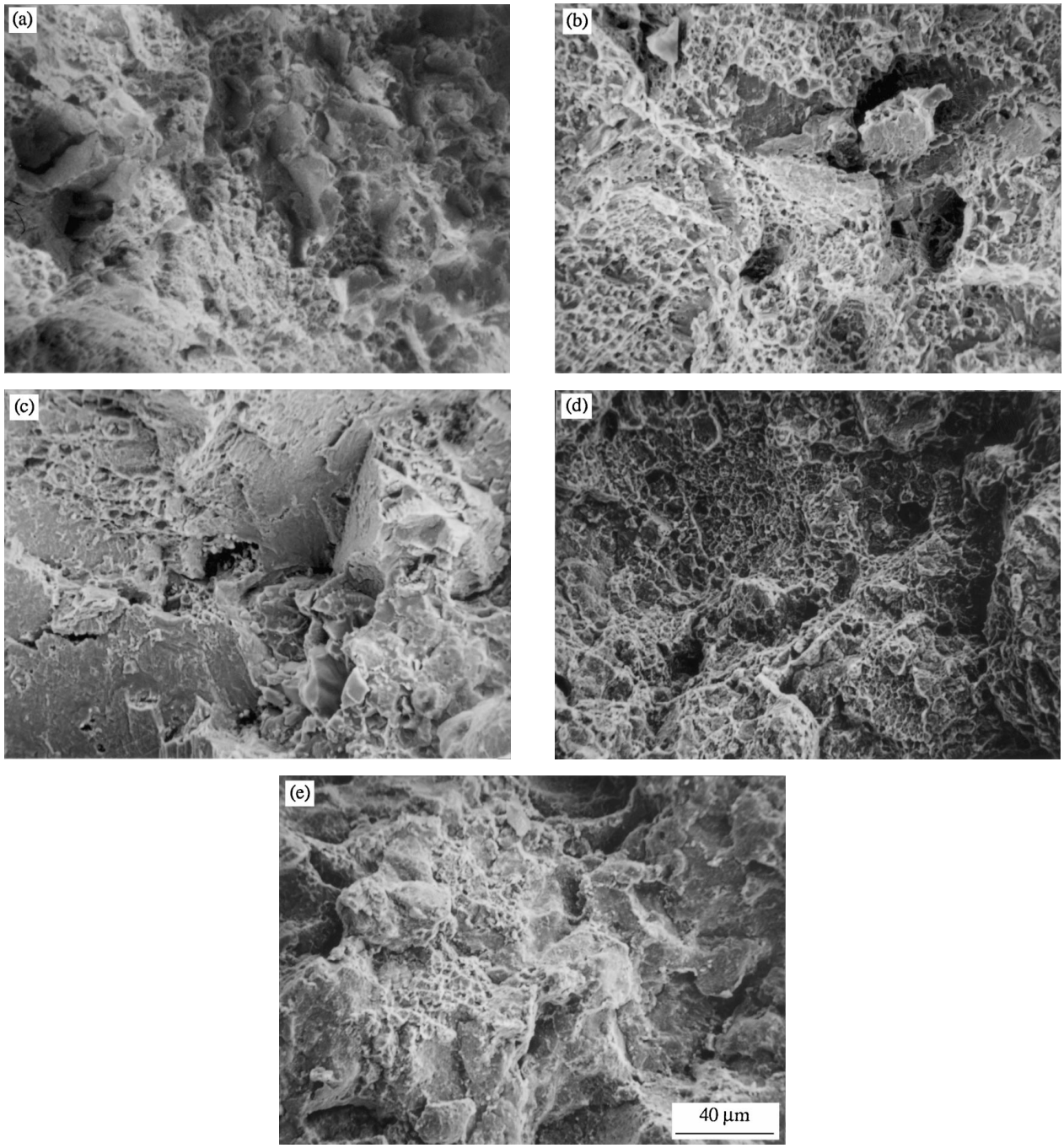

Figure 21 SEM micrographs of the material subjected to HIP at 1250 °C and 100 MPa and tested at room and elevated temperatures, showing dynamic embrittlement at moderate temperatures (approximately 700 °C). Testing temperature: (a) room temperature, (b) 600, (c) 700, (d) 800 and (e) 950 °C.

is found. Moreover, SEM examination reveals that the material subjected to HIP at 1330 °C has a very coarse microstructure, while that subjected to HIP at 1250 °C retains a fine microstructure. However, a well identified ductile fracture structure can always be found wherever transparticle fracture occurs in the material subjected to HIP at temperatures $\geq$950 °C. This may suggest that the Cr-containing Ni_3Al intermetallic consolidated with HIP is intrinsically a ductile material.

The fracture surfaces of the material subjected to HIPed at high temperatures (1250 and 1330 °C) and tested at low temperatures exhibit a transgranular, ductile dimple fracture feature. Ductile rupture via dimples can also be found in the 1250 °C HIP material tested at 800 °C. A transgranular, quasi-cleavage fracture morphology is observed only in the material tested at 950 °C, or at a temperature where dynamic embrittlement occurs in tensile testing, see Fig. 21c. However, a brittle transgranular cleavage fracture feature can be seen in the material subjected to HIP at 1330 °C and tested at temperatures $\geq$600 °C.

Based on tensile-testing results and SEM fractographic examination of the HIP material, the following concluding remarks can be made. A HIP temperature of 850 °C is certainly improper to consolidate the powder, as the mechanical properties of the consolidated material are very poor and fracture is fully in interparticle mode, due to a very low relative density and a small particle contact area.

HIP temperatures between 950 and 1150 °C are insufficiently high. Although the material subjected to HIP at these temperatures already has a reasonably high

(98.5% at 950 °C) or a nearly full (≥99.75% for the others) relative density and a very fine microstructure, interparticle bonding is not strong enough, which makes the powder particle boundaries become weak points. The material subjected to HIP under these conditions has high plastic-deformation resistance, as indicated by a high yield strength, because of its fine microstructure. After yielding, the material undergoes certain homogeneous plastic deformation and final fracture starts at the original particle boundaries because of weak interparticle bonding.

The HIP temperature of 1250 °C gives the most satisfactory results of consolidation, in terms of microstructure and mechanical properties. The material shows the highest resistance to tensile fracture, due to a homogeneous fine substructure and sufficiently strong interparticle bonding. A certain coarsening in grain size is expected in this HIP material. However, from SEM fractographic examination it can be deduced that the grain size of this material seems much smaller than that in the 1330 °C HIP material, with deteriorated mechanical properties caused by defect structures formed during HIP and also excessive grain coarsening.

4. Conclusions

This part of the study mainly concerns the effect of HIP parameters on the microstructure and mechanical properties of a Cr-containing Ni_3Al-base intermetallic prepared via the PM route.

Microstructural development in the material during HIP involves a change in its characteristic microstructure from a rapidly solidified, inhomogeneous structure (a mixture of dendritic and equiaxed structures) to a uniformly distributed equiaxed structure and the formation of a disordered γ network phase from the metastably ordered matrix.

The tensile-testing results show that, except for the material subjected to HIP at 850 °C, the yield strength obtained at testing temperatures lower than 750 °C decreases, while the ultimate strength and ductility as well as the yield strength obtained at testing temperatures higher than 750 °C increase with increasing HIP temperature up to 1250 °C.

The tensile strengths and ductility of the material subjected to HIP at 1330 °C are lower than those of the 1250 °C HIP material. An unusual yielding behaviour of the HIP material has been observed, i.e. rising of the yield stress from room temperature to T_p and falling at higher temperatures. With increasing HIP temperature, T_p shifts to a higher temperature. In the present study, we have found T_p of the 950 °C HIP material at approximately 600 °C and the 1330 °C HIP material at approximately 800 °C.

SEM examination of fracture surfaces reveals a transition from interparticle fracture to transparticle fracture with increasing HIP temperature. Moreover, dynamic embrittlement at moderate temperatures has also been observed in the alloy.

It is concluded that, to consolidate the Cr-containing Ni_3Al–X powder with the HIP process, a temperature of 1250 °C is most satisfactory in terms of the microstructure and mechanical properties of the HIP material.

Acknowledgements

The authors are grateful for stimulating discussions with Dr J. Zhou on the results of the work and for his helpful comments on the manuscript.

References

1. P. H. THORNTON, R. G. DAVIES and T. L. JOHNSTON, *Metall. Trans.* **1** (1970) 207.
2. O. NOGUCHI, Y. OYA and T. SUZUKI, *ibid.* **12A** (1981) 1647.
3. K. AOKI and O. IZUMI, *J. Jpn. Inst. Met.* **48** (1979) 1190.
4. C. T. LIU, C. L. WHITE and J. A. HORTON, *Acta Metall.* **38** (1985) 213.
5. A. I. TAUB, S. C. HUANG and K. M. CHANG, *Metall. Trans. A* **15A** (1984) 399.
6. C. C. KOCH, J. A. HORTON, C. T. LIU, O. B. CAVIN and J. O. SCARBROUGH, in "Rapidly Solidification Processing, Principles and Technologies," Vol. IV, edited by R. Mehrabian (National Bureau of Standards, 1983) p. 264.
7. D. J. LOOFT and E. C. VAN REUTH, in "Rapidly Solidification Processing," edited by R. Mehrabian, B. H. Kear and M. Cohen (Claitor, Baton Rouge, 1978) p. 1.
8. P. N. ROSS and B. H. KEAR, in "Rapidly Quenched Metals III," Vol. 1, edited B. Cantor (Chameleon Press, London, 1978) p. 102.
9. Y. W. KIM, W. M. GRIFFITH and F. H. FROES, *J. Metals* **37** (1985) 27.
10. W. WANG and N. J. GRANT, *Int. J. Rapid Solidification* **1** (1984) 157.
11. H. D. HANES, D. A. SIEFERT and C. R. WATTS, Hot Isostatic Pressing, MCIC Report 77-34 (Battelle Columbus Laboratories, Columbus, OH, 1977).
12. H. FISCHMEISTER, *Powder Metall. Int.* **10** (1978) 119.
13. R. LAAG, W. A. KAYSSER, G. GALINSKI and R. MAURER, in Proceedings of the International Conference on Powder Metallurgy PM into the 1990s, London, 2–6 July 1990 (The Institute of Metals, London, 1990) p. 278.
14. A. LAWLEY, in ASTM **STP 979**, edited by B. L. Bramfitt, R. C. Benn, C. R. Brinkman and G. F. Vander Voort (American Society for Testing and Materials, Philadelphia, PA, 1988) p. 183.
15. S. C. HUANG, K. M. CHANG and A. I. TAUB, in Proceedings of the International Conference on Rapidly Solidified Materials, San Diego, CA, 3–5 Feb 1986, edited by P. W. Lee and R. S. Carbonara (American Society for Metals, 1986) p. 225.
16. I. BAKER, J. A. HORTON and E. M. SCHULSON, *J. Mater. Sci.* **21** (1986) 3297.
17. V. K. SIKKA, *MRS Symp. Proc.* **81** (1987) 487.
18. A. I. TAUB and M. R. JACKSON, *ibid.* **58** (1986) 389.
19. R. N. WRIGHT, B. H. RABIN and J. R. KNIBLOE, *Mater. Manuf. Proc.* **4** (1989) 25.
20. J. DUSZCZYK, L. Z. ZHUANG and L. BUEKENHOUT, *J. Mater. Sci.* **33** (1998) 2735.
21. L. Z. ZHUANG, Research Report, Delft University of Technology (February 1990).
22. L. Z. ZHUANG, I. MAJEWSKA-GLABUS, R. VETTER and J. DUSZCZYK, *Scripta Metall. Mater.* **24** (1990) 2025.
23. *Idem, ibid.* **24** (1990) 2083.
24. *Idem*, in Proceedings of the First International Conference on Spray Forming, Swansea, 17–19 September 1990, p. 19.01.
25. W. A. KAYSSER, M. ASLAN, E. ARZT, M. MITKOV and G. PETZOW, *Powder Metall.* **81** (1988) 63.
26. L. Z. ZHUANG *et al.*, Unpublished results, Delft University of Technology (1990).
27. R. W. CAHN, in Proceedings of the Material Research Society Symposium on High Temperature Ordered Intermetallic Alloys, Vol. 81, edited by N. S. Stoloff, C. C. Koch, C. T. Liu and O. Izumi, (Materials Research Society, 1987) p. 27.

Received 9 September 1997
and accepted 3 September 1998